euronoise

On the correlation of the acoustic signal of microphones mounted on a flat plate to the turbulence of an impinging jet

Christoph Reichl[a], Michelle Boeck[a], Wolfgang Tilser[a], Hermann Lang[a], Klaus Haindl[b], Friedrich Reining[b] and Martin Opitz[b]

[a]Arsenal Research - Austrian Research Centers, Giefinggasse 2, 1210 Wien, Austria
[b]AKG Acoustics GmbH, Lemboeckgasse 21-25, 1230 Wien, Austria
christoph.reichl@arsenal.ac.at

A turbulent circular free stream jet is generated using an axial symmetric fan driven by a brushless actuator with variable frequency leading to typical core-velocities of around 10 m/s (Re = 99000). The flow is propagated through a pipe system significantly damping the noise from the fan. Turbulence is generated using different sets of turbulence generators in the pipe consisting of meshes, rods, cubes and spikes. The turbulent flow field downstream of the pipe outlet is measured using two-axis hot wire anemometry with a temporal resolution of a minimum of 48 kHz. The CTA probe is positioned using an automated three-axis traversing system. Microphones located at freely adjustable positions are used to capture the acoustic radiation and the wall pressure fluctuations. CFD calculations are performed for the different turbulence generators and compared to the acoustic and CTA signals. An important aspect of the work is the simultaneous recording of both the CTA- and the acoustic signals in the experimental and numerical approach. This allows for the calculation of correlation patterns between turbulence and the acoustic signals. The generation of free stream turbulence in a controlled way and its correlation to downstream pressure fluctuations is the primary aim of the work.

1 Introduction

A turbulent circular free stream jet is generated using an axial symmetric fan driven by a brushless actuator with variable frequency leading to typical core-velocities of around 10 m/s (Re = 99000). The flow is propagated through a pipe (radius = 80.5 mm). Turbulence is generated using different sets of turbulence generators [2, 3, 4] in the tunnel (length approx. 2.5 m) consisting of meshes, rods, blades and spikes. The turbulent flow field downstream of the pipe outlet is measured using two-axis hot wire anemometry [1] with a temporal resolution of 48 kHz. The CTA probe is positioned using an automated three-axis traversing system. The turbulent jet impinges on a wall in the distance of 0.55 m from the pipe outlet. 12 Microphones are positioned on a flat plate mounted on the wall in the center-line of the jet. CFD (computational fluid dynamics) calculations are performed for the different turbulence generators and compared to the CTA signals. An important aspect of the work is the simultaneous recording of both the CTA- and the microphone signals. This allows for the calculation of correlation patterns between turbulence and the acoustic signals. The generation of free stream turbulence in a controlled way and its correlation to downstream pressure fluctuations is the primary aim of the work.

2 Numerical Simulation

The numerical analysis have been performed on a hybrid mesh consisting of tetrahedral cells in the region of the turbulence generators (see figure 2) and a prismatic / hexahedral mesh in the up- and downstream area. Mesh sizes of 2 mm at the turbulence generator core lead to typical cell counts of 3 million cells). Best results have been achieved by applying a turbulent velocity profile at the tube inlet and fixing the turbulent kinetic intensity to a value of 2.6 %. The fluid leaves the calculation area through the cylindrical surface and its base plane (see figure 2). The jet impinges on the opposite circular area of the cylinder, which is defined as a hard wall. Steady CFD calculations leading to acceptable low numeric residuals were not possible for all turbulence generators. Sharp blades caused very high fluctuating fields, which could not be captured by a steady solver. Comparing experimental and numerical results, the RNG formulation of the k-ε model gave best agreement.

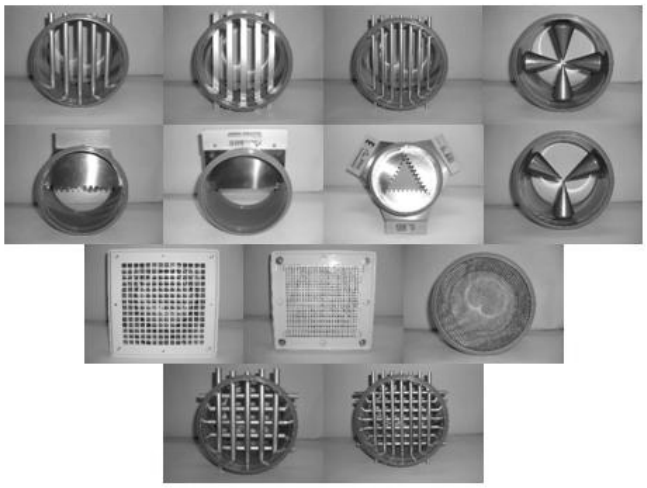

Fig.1 Different turbulence generators consisting of rods, blades, spikes and meshes. They can be mounted on top of the tunnel outlet. First row: TG01, TG08, TG02, TG05; Second row: TG07, TG10, TG09, TG06; Third row: TG11, TG13, TG12; Fourth Row: TG04, TG03

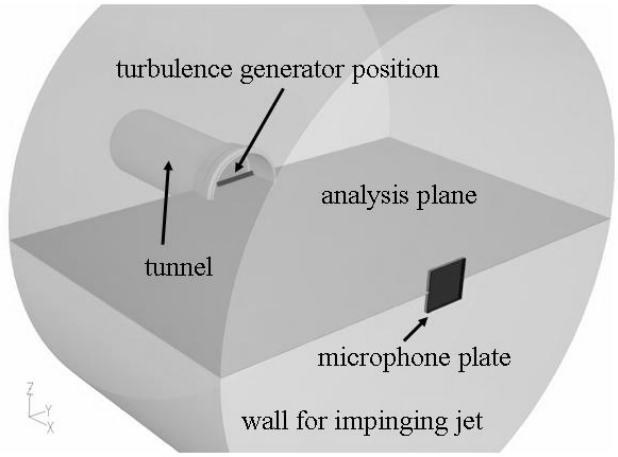

Fig.2 Geometry for the CFD simulation. A circular jet impinges on a microphone plate mounted on a wall. Turbulence generators can be applied in the outlet region of the tunnel.

The differences have been found to be most pronounced in the near wall region at the microphone plate. Figure 3

shows the turbulent kinetic energy on the analysis plane for a turbulence generator with 4 spikes (TG05).

Fig.3 Turbulent kinetic energy [m^2/s^2] for a turbulent generator with 4 spikes. The simulations are performed using a steady kε-RNG model (grey scale range from 0 to 1).

3 Experimental Results

Signals from the 2-axis CTA (constant temperature anemometer) have been recorded simultaneously with 12 microphone signals with a sampling rate of 48 kHz. The data were acquired in the analysis plane on 492 points (streamwise tunnel direction x: 12 points, perpendicular crosswise direction +y: 41 points). All signals (CTA, microphone) have been scaled by their corresponding calibration values. For the spectral analysis they have been further numerically filtered (low pass filter 20 kHz), DC subtracted and Fourier transformed. In the figures always the normalized, absolute squared value, which is multiplied by a factor of two to account for the positive frequency space, is shown. CTA and acoustic FFT signals are displayed in a logarithmic scale, for acoustic signals, the sound pressure level was calculated using a reference pressure of 20 µPa, for CTA signals the reference value was set to 1 m^2/s^2. Figure 4 gives an overview of the evolvement of turbulent velocity field for different x-positions. The data was recorded in the center (y=z=0 m) of the jet directly pointing towards the microphone plate.

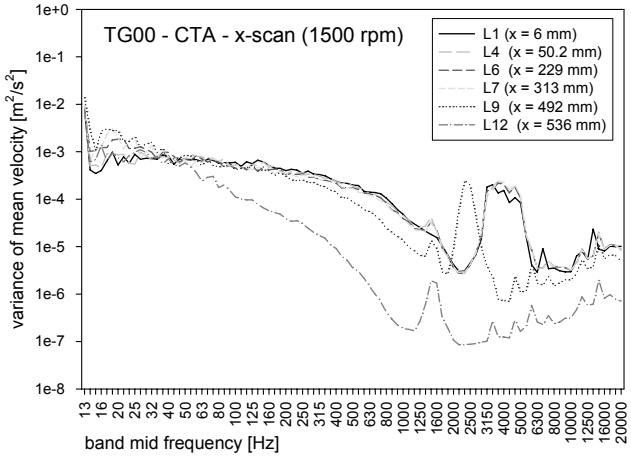

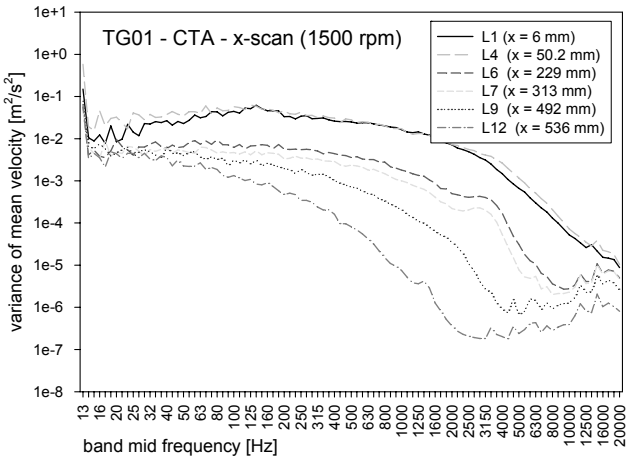

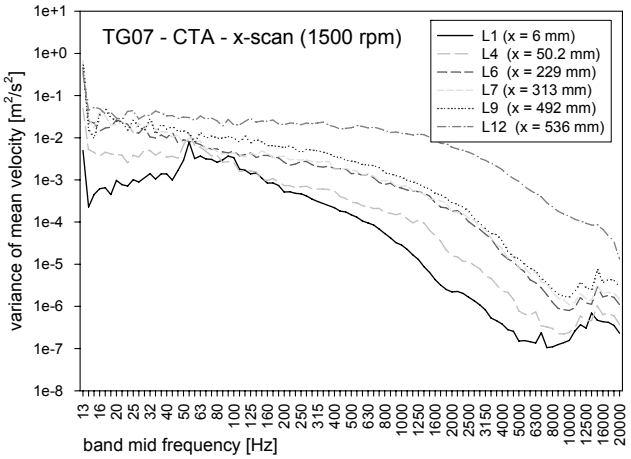

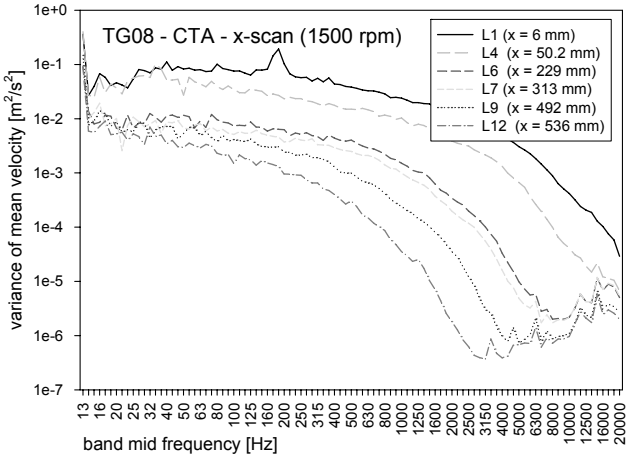

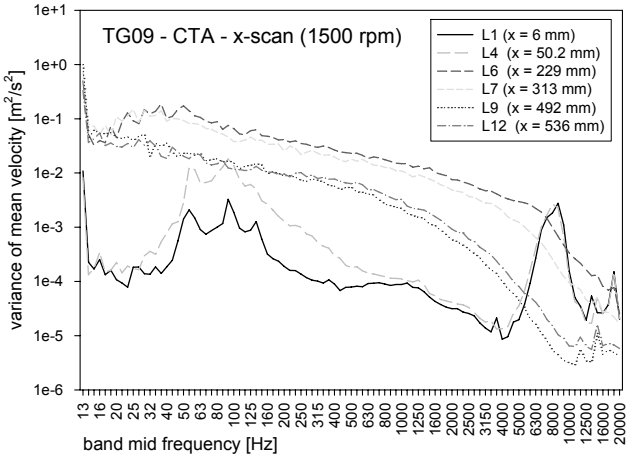

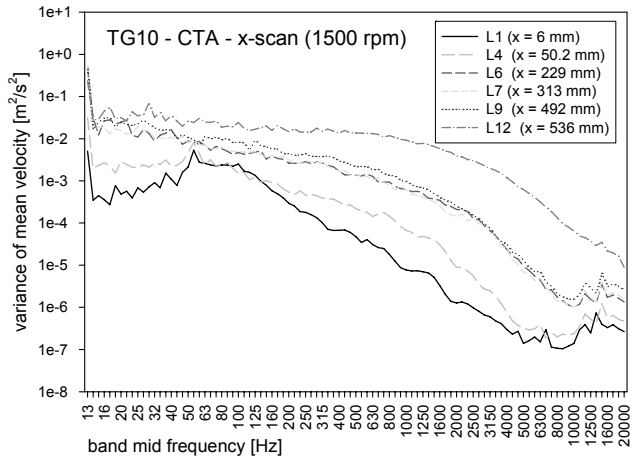

Fig.4 Development of the turbulent flow field of different turbulence generators, showing the variance of the mean velocity based on the CTA signal. The area below the different curves correspond to the variance of the mean velocity.

Different spatial evolvement of the frequency distributions can be observed applying different turbulence generators. Often some spectral peaks can be found between 50 Hz and 160 Hz in the direct vicinity of the turbulence generator (L1). The spectra then generally start a deep slope down in sound pressure level from around 1000 Hz towards higher frequencies.

Acoustic measurements for all turbulence generators were performed downstream of the tube outlet (distance 55.5 cm) directly on the plate and offaxis (angle of 60° to the x-axis). Figure 5 shows the offaxis acoustic signal for a fan rotation frequency of 1500 rpm. The largest contribution lies in the 250 Hz range, almost no contribution can be seen in the lower frequency range. The signal is almost independent from the turbulence generator placed in the tube and comes primarily from the sound radiation of the fan.

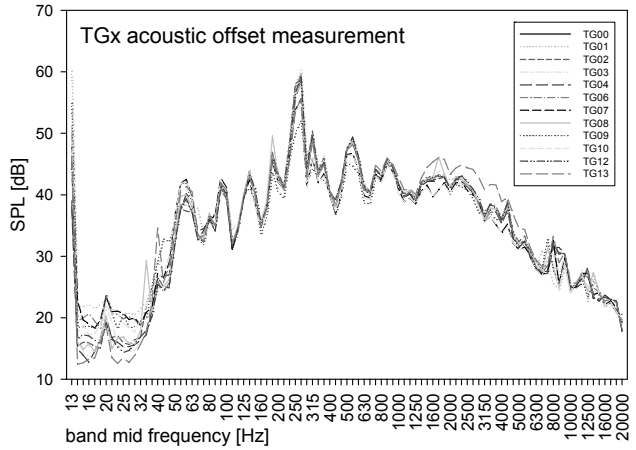

Fig.5 Acoustic measurements downstream of the tube outlet (distance 55.5 cm) and offaxis (angle of 30° to the x-axis). The fan speed was fixed to 1500 rpm.

Figure 6 – 8 compare parts of the recorded time-series of CTA and microphone signal. Periods of fast and slow fluctuations correlate (see fig. 8), an exact match (even considering a slight offset due to time shift between CTA and MIC position) of the waves cannot be seen. The signals of the microphones MIC10 and MIC12 which are horizontally separated by about 2 cm are shown in fig. 8.

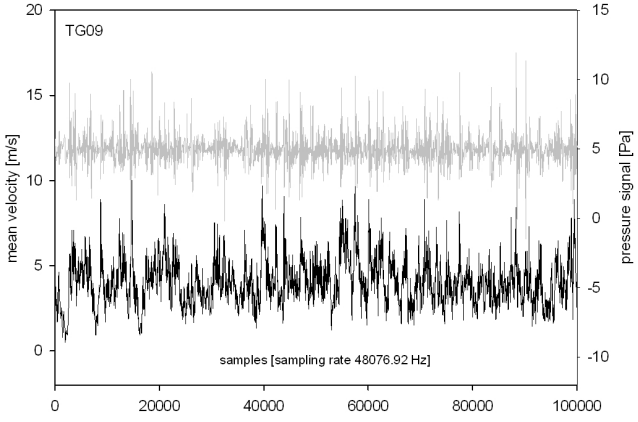

Fig.6 Comparison of the simultaneous recorded signals of the microphone MIC12 and the CTA positioned 5mm in front of the microphone for turbulence generator TG09. The gray curve corresponds to the microphone signal (right axis), the black curve to the mean velocity of the CTA (left axis).

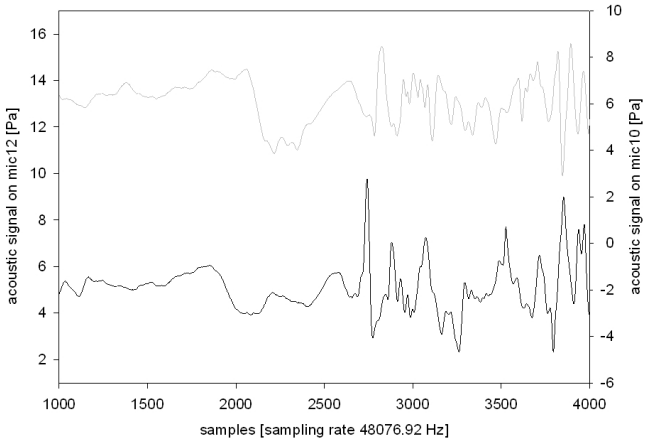

Fig.7 Simultaneous recording of the pressure signal at two microphones on the plate in the impinging jet range. The distance of the two microphones in y-direction is about 2cm. Showing overall similar behaviour (fast and slow fluctuations), the two curves are not matching, showing differing local pressure fluctuations at different positions on the plate.

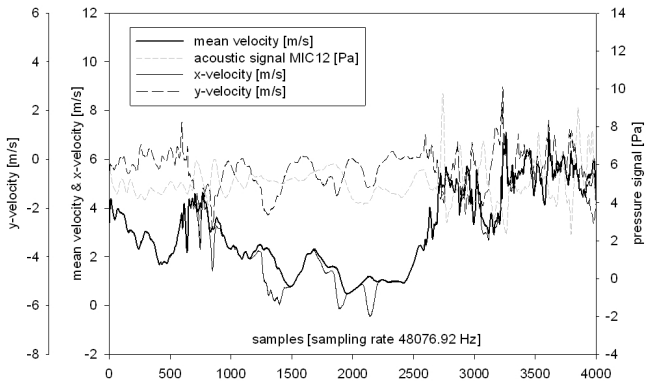

Fig.8 Comparison of the simultaneous recorded signals of the microphone MIC12 and the CTA positioned 5mm in front of the microphone (turbulence generator TG09). Shown are the mean velocity, the x- and the y-velocity components.

To analyse the correlation between microphone signal on the plate (MIC 12) and the CTA signal 5mm in front of the microphone, fig. 10 and fig. 11 show overviews of the frequency spectra for different turbulence generators.

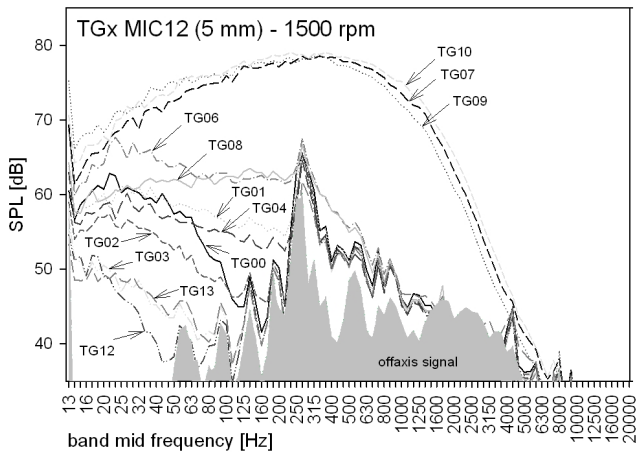

Fig.9 Comparison of the frequency spectra of the microphone MIC12 for the different turbulence generators (TGx). The signal was recorded at the center of the plate (y~1cm, z = 0), where the turbulent jet impinges on the microphone plate. The gray area is the maximum signal of the acoustic offset measurement for the different TGx.

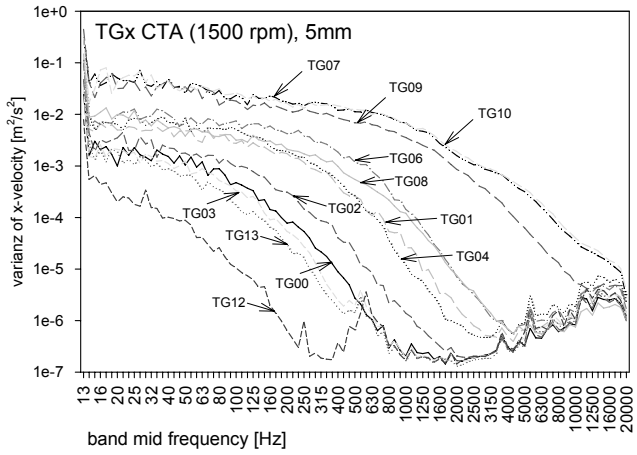

Fig.10 Comparison of frequency spectra of the CTA signal (mean velocity) for the different turbulence generators (TGx). The signal was recorded 5mm in front of the microphone MIC12, where the turbulent jet impinges on the microphone plate.

The microphone signals (fig. 9) clearly show large frequency content in the range up to 200 Hz, where no sound contribution from the fan (grey area) is present. The CTA signals (see fig. 10) show their large spectra content in this low frequency range. Comparing the different turbulence generators, a good agreement in the power and in the width of the spectra can be found.

For some turbulence generators (TG07, TG09, TG10) an even broader (and higher) spectrum is observed completely masking the fan noise (which is also directly propagating through the tube towards the microphone plate). Only part of this frequency range can be seen in the CTA signal and thus be attributed to the local velocity fluctuations at the plate.

Fig. 11 compares frequency spectra of the microphones on the plate (MIC 12) with the local x-velocity fluctuations 5mm in front of the microphone for different turbulence generators TGx.

For each generator TGx, microphone and CTA signals for 5 different rotation frequencies (500, 750, 1000, 1250 and 1500 rpm) of the fan have been measured.

If no turbulence generator is inserted into the tube (TG00) and for some "quiet" turbulence generators the noise from the fan can readily be seen in the spectra.

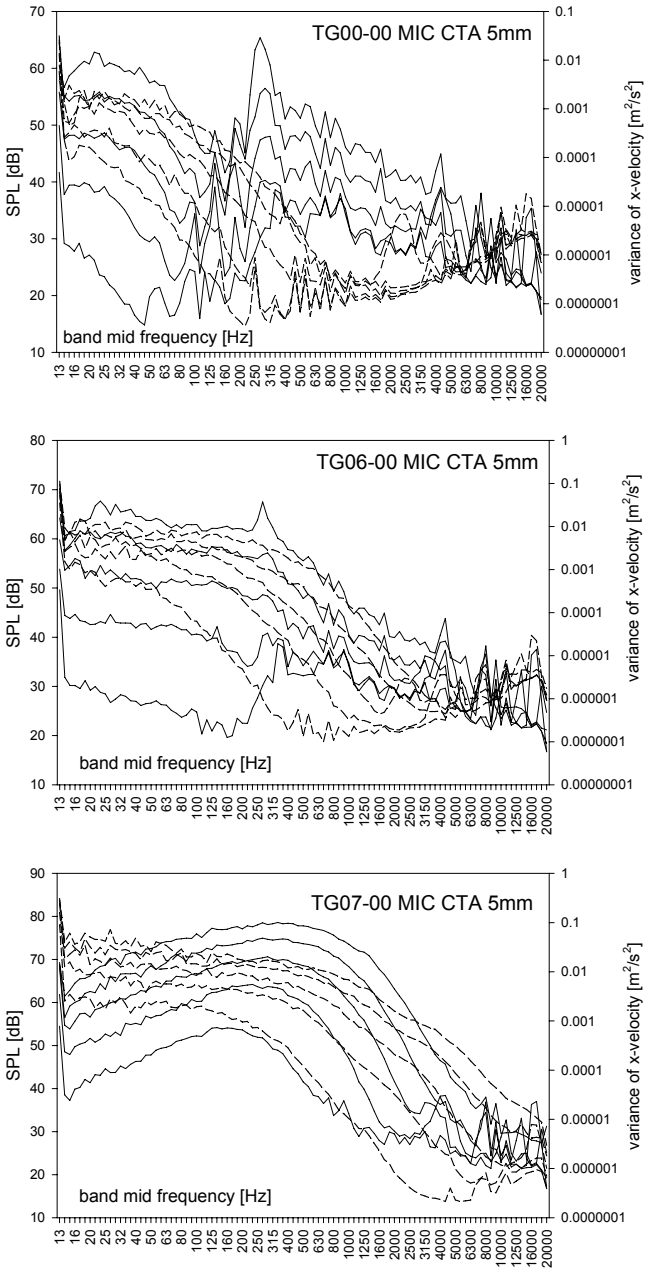

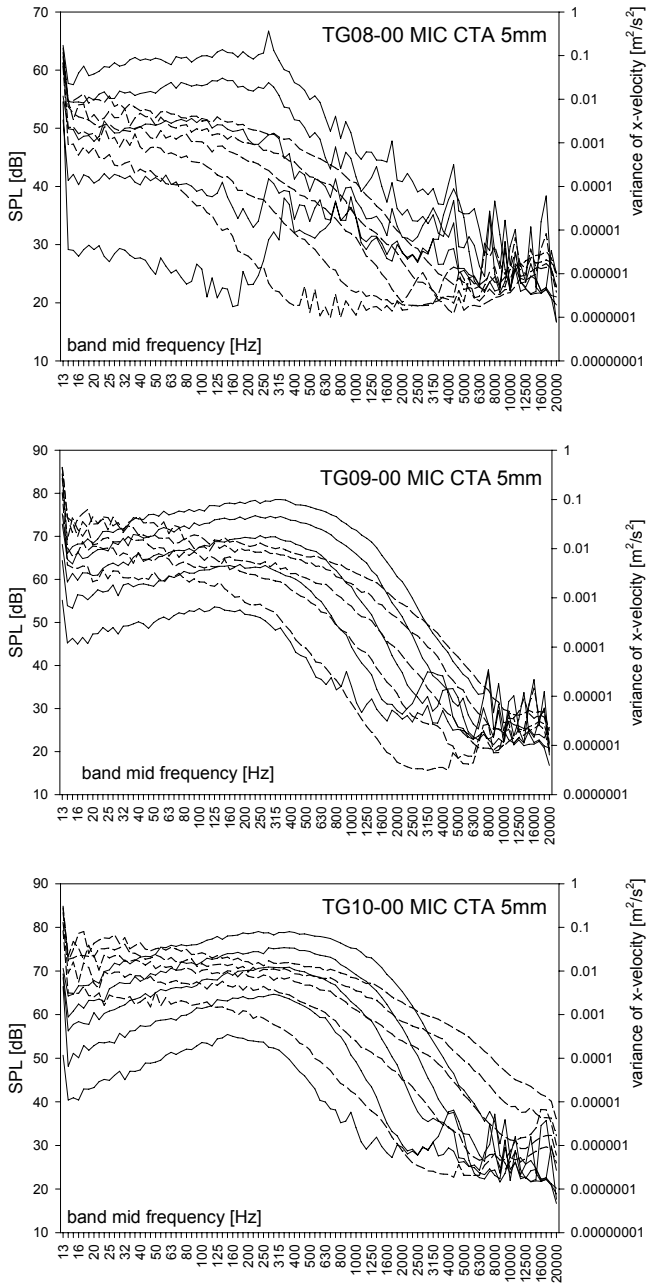

Fig.11 Comparison of the frequency spectra of the microphone signals (bold lines, MIC 12) to the CTA spectra (dashed lines) for different turbulence generators TGx. The CTA signal was recorded 5mm in front of the microphone MIC12, where the turbulent jet impinges on the microphone plate. The five different sets correspond to the fan speed frequencies of 500, 750, 1000, 1250 and 1500 rpm.

5 Conclusion

Steady CFD simulations can give trends but are not ideally suited for quantitative analysis as they are not able to capture the inherent transient flow patterns. The RNG formulation of the k-ε model compared best to the experimental data (streamwise and crosswise velocity, turbulent kinetic energy). Differences in the models are most pronounced in the stagnation area of the impinging jet at the wall. For some turbulence generators (blades), a steady solution could not be achieved.

Correlations between turbulent velocity fields and microphone signals have been investigated for different turbulence generators. Larger turbulence coincides with larger pressure fluctuations, the full frequency behaviour, however, could not always be reproduced. The reasons may lie in additional acoustic incoming waves, which can be attributed to dipolar and quadrupolar sound sources as well as vibrations of the turbulent generators.

Broader CTA spectra, however, coincide well with broader signals at the microphones.

Transient CFD simulations (DES) will be employed to provide frequency spectra for comparison to the experimental data. Furthermore, the correlation between simulated local velocity fluctuations and pressure fluctuations at the wall can be investigated. These results will also be compared to the experimental correlation, as CTA and microphone signals have been recorded simultaneously. The 12 microphone signals also allow for spatial correlation analysis.

Acknowledgements

We want to express our gratitude to the Austrian Science Foundation (FFG) supporting this work in the framework of the Bridge project TUNICA.

References

[1] Bruun, H. H., “Hot-Wire Anemometry: Principles and Signal Analysis”, Publisher: Oxford University Press, USA (June 8, 1995), ISBN: 0198563426

[2] Counihan, J., “An improved method of simulating an atmospheric boundary layer in a wind tunnel”, *J. Fluid Mechanics*, vol. 3, pp. 197-214, 1969.

[3] Guimaraes, J. H. D., dos Santos, S. J. F., Su, J., Silva Freire, A. P., “Large artificially generated turbulent boundary layers for the study of atmospheric flows”, *Proceedings of the 15th Brazilian Congress of Mechanical Engineering (COBEM99)*, Aguas de Lindoia, 1999

[4] Hunt, J. C. R., Fernholz, H., “Wind-tunnel simulation of the atmospheric boundary layer”: a report on Euromech 50, J. Fluid Mechanics, vol. 70, pp. 543-559, 1975.

[5] Jovanovic, J., ”The Statistical Dynamics of Turbulence”, ISBN 3-540-20336-2 Springer Verlag Berlin Heidelberg New York, 2002

[6] Ramezanpour, A., Shirvani, H., Mirzaee, I, ”Heat transfer modelling of slot jet impinging on an inclined plate”, *Heat Transfer VIII*, B. Sundén, C. A. Brebbia & A, Mendes (Editors)